Hydraulic conclusions from chemical considerations: groundwater in sedimentary environments in the central part of the Pannonian Basin, Hungary

Irén Varsányi · Lajos Ó. Kovács · András Bálint

Abstract Hydro-chemical and isotopic data from different aquifers in the Great Hungarian Plain (the central part of the Pannonian Basin) were evaluated down to a depth of 2,740 m. The chemical and isotopic composition of water is influenced by its origin and by chemical and mixing processes. The analytical data and chemical considerations, together with geology, pressure conditions and evolution history of the area, explain the evolution of the subsurface water. Most of the samples are of meteoric origin, but there were some samples with a non-meteoric contribution, as indicated by the water stable isotopes, and these were identified as seawater trapped during the sedimentation in Lake Pannon. The sea contribution is traceable by the shifts in $\delta^{18}O$ and δ^2H and the chemical composition of the water, and is explained with an upward-driving force. Chemical considerations and spatial variability of the dissolved components suggest that distinct water bodies, each with a specific origin and chemical evolution, can be separately identified. Although in the Quaternary layers there are water bodies that can be considered to display complete flow systems (from recharge to discharge), in most water bodies present infiltration was not identified. The lack of recent recharge to several water bodies in various places and depths suggests a separation of the recharge and the discharge that occurred not in space, but in time. A possible explanation of the cessation of recharge is a significant change in the hydraulic circumstances, probably the surface elevation.

Keywords Hydrochemistry · Hydrodynamics · Stable isotopes · Basin evolution · Hungary

I. Varsányi (✉) · A. Bálint
Department of Mineralogy, Geochemistry and Petrology,
University of Szeged, P.O. Box 651, Szeged, H-6701, Hungary
e-mail: varsanyi@geo.u-szeged.hu
Tel.: +36-62-544641

L. Ó. Kovács
Hungarian Office for Mining and Geology, P.O. Box 95, Budapest, 1590, Hungary

Introduction

The chemical and isotopic composition of subsurface water is influenced by its origin, by the type of rocks accommodating the water, and by the hydrogeological character of the study area. The relationship between the hydro-chemical and flow patterns of subsurface water has long been known about and documented by many authors. Chebotarev (1955) described the influence of the hydrodynamic character of reservoirs on the geochemical type of subsurface water. He recognized a regional $HCO_3^- \rightarrow SO_4^{2-} \rightarrow Cl^-$ sequence of the dominant anions, and concluded that this sequence was the result of the hydro-chemical evolution of subsurface water along the flow path. He established that variation of salinity was a function of flow rate. Back (1966), who published a detailed study about the relationship between the hydro-chemical facies and groundwater flow in the Atlantic Coastal Plain (USA), concluded that a hydro-chemical facies reflects both the chemical processes operating within a particular lithological framework and the pattern of water flow, which is entirely controlled by the lithology of the deposits through which the water flows. Back (1966) verified that groundwater flow played an important role in the distribution of the hydro-chemical facies. Back and Hanshaw (1970), in studying the carbonate peninsulas of Florida (USA) and Yucatan (Mexico), found a direct connection between the specific conductivity of groundwater and the potentiometric surface. The lowest conductance was found in the area with the highest potentiometric surface and the greatest recharge, and it increased downgradient. In the Ross Creek Basin (Canada), Ophori and Tóth (1989) found a correlation between the water flow and the hydro-chemical pattern. They established that low total dissolved solid content, a high Ca^{2+} to Mg^{2+} ratio, and low SO_4^{2-}

concentrations are characteristic in the recharge areas, and found the opposite conditions in the discharge areas. They concluded that water chemistry may relate to both the hydraulic regimes (inflow, throughflow, outflow) and the type of the flow system (local, intermediate, regional). A flow system was defined by Tóth (1963) as a coherent, three-dimensional (3D) unit of groundwater flow with one recharge and one or more discharge areas. Stuyfzand (1999) used hydrochemistry to identify the recharge area of groundwater, flow pattern and degree of mixing. He defined hydro-chemical facies as a chemically homogeneous type of water, and the water body (hydrosome) as a coherent, 3D unit of groundwater with a specific origin. Within a certain water body the chemical composition of subsurface water varies in time and space, due to changes in recharge composition, flow patterns, or water–rock interaction. Consequently, a water body consists of different hydro-chemical facies, each with a homogeneous chemical character. Stuyfzand (1999) also demonstrated in fresh coastal-dune groundwater (Netherlands) that the evolution in the direction of the groundwater flow within water bodies was from acidic to basic, from oxic to anoxic, from fresh to brackish, and from strong to no fluctuation in terms of hydrochemistry.

The purpose of this study is to find the relationship between the water chemistry and flow pattern of subsurface water in sedimentary environments. The fundamental questions are: (1) Does a specific chemical pattern indicate a specific hydraulic regime? (2) Within a given hydrologically defined underground domain, is the water chemistry indicative of the evolution of the infiltrating water?

Geological background

The study region covers about 22,000 km^2. The location of the study area in the eastern part of Hungary is presented on a sketch map (Fig. 1a). The study area represents the central part of the Pannonian Basin, which is filled with Neogene sediments. The history of the Pannonian Basin is tightly connected to the history of Lake Pannon, which was formed at the beginning of the Late Miocene with the separation of the Paratethys Sea from the oceans. In the Late Miocene, sedimentation initially occurred in deep and brackish water, and later in freshening and shoaling water (Horváth and Pogácsás 1988). Subsidence throughout the area during the early stage of the Late Miocene (Pannonian *s. str.*, henceforward Pannonian) is supposed; the rate of subsidence was diverse, resulting in a highly variable sediment thickness. In the deepest zones, turbidite was formed in the deep brackish water. Deltas were prograding from the N/NW and N/NE to the S/SE and S/SW, respectively. The freshening and shoaling environment is represented by the fine-grained delta slope facies at the end of the Pannonian. By the beginning of the Pontian (later in the Late Miocene), the subsidence slowed down, and the gradual infilling of the basin was almost completed. Upper delta-slope and delta-plain followed by alluvial plain

facies are characteristic of the Pontian. The complete desiccation of Lake Pannon coincided with the Miocene-Pliocene boundary. In the Pliocene, tectonic inversion and uplift became dominant establishing conditions for meteoric infiltration. The tectonic movements at the Pliocene-Quaternary boundary were significant (Nagymarosy and Hámor 2012). During the Quaternary, the subsidence rate increased in the central part of the basin while uplift continued in the flanks (Horváth and Cloetingh 1996). The top of the Pliocene and the Quaternary are represented by variegated lacustrine, fluvial and terrestrial sequences. The tectonic events resulted in sub-basins with highly variable sediment thicknesses, and highs between them. Two characteristic cross-sections, one for an area above elevated basement and one for two deep sub-basins, are shown in Fig. 1b and c, respectively.

According to Juhász et al. (2002), the evolution of the Pannonian Basin determined its hydrologic history, as well. The formation of the core complex and the uplift of the crystalline basement were associated with meteoric water infiltration along shear zones into the Pannonian layers covered by water. Later on, hydrologic inversion occurred, due to the thermal subsidence of the basin, and this led to a hydrologic system with no downward water flow from the surface.

In the study area, there are three main aquifers: the pre-Pannonian, the Szolnok Formation (middle of the Pannonian) and the Nagyalföld (corresponding to the Újfalu and Zagyva Formations and the Quaternary layers), and two aquitards were identified—the Endrőd (at the bottom of the Pannonian) and the Algyő Formations (at the top of the Pannonian). The main relevant features of the studied stratigraphic units are given in Fig. 2.

Processes controlling the chemical and isotopic compositions and the relevant chemical considerations

Water stable isotopes

Correlation of the $\delta^{18}O$ and δ^2H values can help to establish the origin of subsurface water and the temperature during infiltration. The origin is shown by the location of isotope δ values in the $\delta^{18}O$ vs δ^2H diagram. The samples on the local meteoric water line (LMWL) are considered to be of meteoric origin. Those samples which deviate from the LMWL could originate from other sources, for example, seawater, and could go through evaporation or isotope exchange reaction at high temperature and they may be mixed waters consisting of meteoric and non-meteoric end-members. The position of the samples on the LMWL is indicative of the temperature of the infiltration. The water depleted in ^2H and ^{18}O isotopes (more negative δ value) infiltrated in a colder period, and the enriched (less negative δ value) in a warmer period (Clark and Fritz 1997). The relationship between noble gas temperature and the water stable isotope δ value can be used to calibrate a local stable isotope thermometer (Varsányi et al. 2011). The validity of
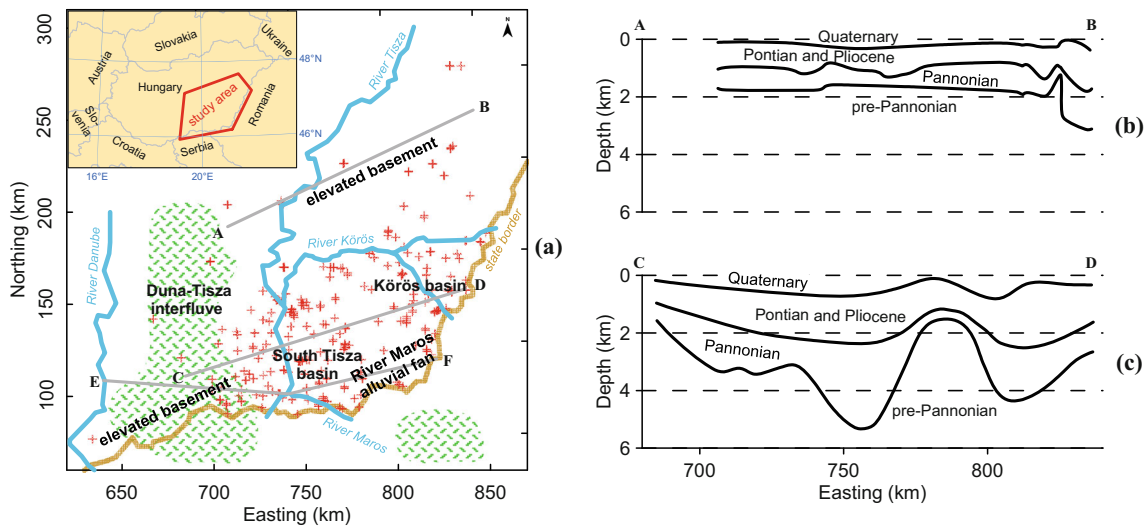
Fig. 1 Location and structure of the study area. **a** Index and sketch map of the study area with location of the sampled wells (*red crosses*) and traces of the cross-sections, **b** Cross-section of an area above elevated basement. **c** Cross-section of deep sub-basins. *A–B* and *C–D* are traces of characteristic cross-sections in this paper. *E–F* is the trace of the hydraulic cross-section by Tóth and Almási (2001). Patterned areas are the recharge areas defined by Erdélyi (1979)

the thermometer is limited to the time span given by the age of the water samples involved in the calibration.

Chemical processes

To interpret the hydro-chemical data and to find an explanation of the observed chemical patterns and their relationship to the alteration of paleo-geographic circumstances, the relevant chemical reactions have to be identified and characterized. In the study area, the main sources of the major dissolved components in the subsurface water are dissolution of silicates and other

minerals of simple structure (for example, carbonates or gypsum) initiated by the production of CO_2, and ion exchange. The chemistry of these processes is summarized briefly in the following.

Types of dissolution

There are two types of dissolution: one type reaches chemical equilibrium and this type of chemical reaction is thermodynamically controlled; and the other type, which proceeds during the whole contact time between water and minerals, is controlled kinetically. The concentrations of

Epoch	Stage[a]	General facies[a]	Formation[b,c,d]	Tectonic event[e]	Hydrochemical indications for stratigraphy (present study)
Quaternary		continental, fluviatile		in different basin parts uplift or subsidence	mirror image of mono- and bivalent cations along flow path
Pliocene				late tectonic inversion and uplift	
Miocene (Late)	Pontian	freshwater, lacustrine-fluviatile	Zagyva, aquifer, k=1000 md		NaHCO₃-type formation water of meteoric origin
			Újfalu, aquifer, k=1000 md	post-rift subsidence	
	Pannonian	brackish	Algyő, aquitard with aquifer lenses, k=1-10 md		formation water of sea origin with high Cl⁻, and with Cl⁻ to Br⁻ ratio similar to that of the seawater
			Szolnok, aquifer, k=10-100 md		
			Endrőd, aquitard, k=0.1 md	early tectonic inversion	

Fig. 2 Summarized geologic information for the study area. *k* stands for permeability. *a* Horváth and Pogácsás (1988); *b* Magyar (2010); *c* Tóth and Almási (2001); *d* Nagymarosy and Hámor (2012); *e* Sacchi and Horváth (2002)

the products are determined either by the equilibrium constant of the relevant chemical reaction or by the contact (residence) time.

In natural water the major cations are Ca^{2+}, Mg^{2+} and Na^+. The primary source of Ca^{2+} and Mg^{2+} is the equilibrium dissolution of carbonate minerals. The concentrations are constrained by the temperature-dependent dissolution/precipitation equilibrium, which, at constant temperature, is determined by the equilibrium constant (K) of the relevant reactions. For example, the calcite dissolution is:

$$CaCO_3 + CO_2 + H_2O \leftrightarrow Ca^{2+} + 2HCO_3^- \qquad (1)$$
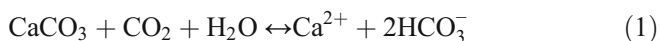
$$K = \frac{[Ca^{2+}][HCO_3^-]^2}{p_{CO_2}} \qquad (2)$$

The equilibrium dissolution of minerals of simple structure is independent of the amount of minerals available in the sediments and the duration of the water–rock interaction. As the equilibrium constant (K) is constant, with increasing partial pressure of CO_2 (p_{CO2}) the concentration of dissolved ions increases (see Eq. 2).

The main source of Na^+ is the weathering of primary silicates containing sodium, which is a kinetically controlled reaction. This reaction produces dissolved H_4SiO_4, Na^+ and secondary (clay) minerals. During weathering, equilibrium is not reached and the reaction proceeds as long as the silicates are available in the sediment. The concentration of dissolved components is proportional to the duration of the water–rock interaction, if all other circumstances are constant: the longer the contact time, the higher the concentration of Na^+. The total amount of CO_2 available during the whole contact time promotes the weathering of silicates through H^+ production. Although there may be various source of the CO_2, in the study area it originates from the root zone in the soil, and in the deeper layers additional CO_2 is provided through evolution of sediment organic matter, as it was reported elsewhere (Varsányi et al. 1997). During the evolution, together with the loss of the carbon-containing functional groups of the sediment organics, CO_2, dissolved organic matter and NH_4^+ were produced and enrichment of the heavier carbon isotope in the bicarbonate was detected. The NH_4^+, bicarbonate (as alkalinity) and $\delta^{13}C$ directly correlate with each other. As this is a kinetically driven reaction, the amount of the products of the reaction is proportional to the duration of exposure.

The main difference between the two types of dissolution reaction is that the carbonate dissolution/precipitation is controlled by the actual partial pressure of CO_2 according to Eq. (1), whereas the concentration of Na^+ is determined by the total amount of CO_2 dissolved during the whole time of the exposure. In absence of secondary reactions, kinetically driven weathering that depends on the duration of exposure (residence time) may provide much higher concentrations of dissolved ions than equilibrium dissolution.

Certain trace elements, such as Li, Rb, Cs, Mn and Mo, which are progressively released by kinetically controlled weathering reactions, are used as residence time indicators (Edmunds and Smedley 2000). These are not affected by solubility control, which would limit their concentrations; hence, they are used for estimating the contact time in certain environments.

Ion exchange

Along the flow path, the opposite and equivalent change in the dissolved major mono- and bivalent cations suggests ion exchange reactions. Ion exchange takes place when an initial aqueous solution in equilibrium with a solid phase containing clay minerals is displaced by flushing water in which the ratio of the major cations are different from those of the initial water. First, the initial water forms an ion exchange complex on clay minerals. The dissolved ions and exchange complex are in equilibrium with each other, and the flushing water disturbs this equilibrium. Because of their interaction, both the flushing water and the ion exchange complex are continuously altering and a set of equilibriums evolves along the flow path. Different retardation of the cations on clay minerals results in a characteristic chromatographic pattern of the dissolved ions along the flow path (Appelo and Postma 1993); thus, the direction of the water flow is detected by the development of the chromatographic pattern. The pattern changes with time, until the displacing water entirely flushes both the initial water and the exchange complex belonging to the initial water. To start up ion exchange and to develop the characteristic ion exchange pattern, alteration (which initiates recharge) is necessary. This alteration is probably the change of surface relief, which results in a modification of the hydraulic circumstances. In a certain area, two opposite changes may result in the flushing of the original pore content: one is the formation of a topographic high, which henceforward functions as a recharge area, and another is the formation of a surface depression generating an upward flow of deep groundwater. In both cases, the chemical equilibrium between the original pore content and the natural exchanger is disturbed by the flushing water, and a new equilibrium and ion exchange pattern develops along the flow path. It is obvious that in the initial state and in the flushing water the ratios between the concentrations of the major cations have to be different.

Samples and methods

In the present study, hydro-chemical and isotopic data were evaluated in the water located in the upper 2,740 m of the sediments. The samples were collected at the wellheads of producing wells during the sampling campaigns of several projects financed by the Hungarian National Research Fund between 1992 and 2013.

Analyses were performed in the accredited laboratories of the Geological Institute of Hungary (Budapest), Public Health Institute (Budapest), Institute of Nuclear Research (Debrecen), Univ. of Alberta (Canada) and BRGM (France). In situ measurements, major and minor ion and trace element analyses, as well as electrical conductivity, alkalinity, chemical oxygen demand (COD) determinations, and several isotopic techniques were used to determine the concentration of dissolved materials. The samples were analyzed in the laboratory for most chemical compounds within 24 h. Chemical analyses were performed according to the Hungarian Standard Methods (MSZ 448/3-47). Alkalinity, COD and Cl^- were determined by titration, Br^- and NH_4^+ by spectrophotometry in unfiltered samples. Sub-samples reserved for determining cations were filtered with a 0.45-µm membrane filter to remove particles, acidified to pH=2 with ultrapure HNO_3 and measured using Perkin-Elmer Zeeman 500 equipment. $\delta^{18}O$ and δ^2H were measured using the GasBench-II preparation systems based on isotope re-equilibration with CO_2. The results are reported relative to Vienna Standard Mean Ocean Water (VSMOW). Analytical uncertainties of the individual measurements were better than 0.1 and 1 ‰ for $\delta^{18}O$ and δ^2H, respectively. Stable carbon isotope ratios from total dissolved inorganic carbon were measured from CO_2 gas extracted with H_3PO_4. Analyses were performed on a Finnigan Delta S mass spectrometer and are reported relative to the PDB standard with a precision of ±0.1 ‰.

In order to understand the nature of water in the deep (Pannonian) sediments, these data were completed with archival chemical, pressure and elevation data collected from unpublished sources (T. József, University of Alberta, unpublished data, 2001; Almási 2000), and with several additional $\delta^{18}O$ and δ^2H data (Deák 2006).

Results

The chemical composition of about 284 samples, and ^{18}O, ^2H and ^{13}C stable isotopes in 134 of those 284 samples are discussed. Parameters of wells and the interpreted analytical data are summarized in Table S1 of the electronic supplementary material (ESM). The depth of wells ranged from 9 to 2,740 m, and the temperatures at the wellhead ranged from 10 to 98 °C. The samples come from the Pontian, Pliocene and Quaternary layers. In the groundwater up to 30 °C, the major cations are either Ca^{2+} and Mg^{2+}, or Na^+, and the major anion is HCO_3^-. In the geothermal water, the major cation is Na^+ and the major anion is mostly HCO_3^-, but in several samples Cl^- dominates. The electrical conductivity varies from 237 to 21,200 µS/cm; the highest values were measured in the Cl^--dominated samples. The pH ranges from 6.7 to 8.7. COD, similar to the inorganic components, varies widely (from 0.5 to 67 mg/l).

$\delta^{18}O$ values range between −13.35 and −0.36 ‰, δ^2H between −100.23 and −35.06 ‰, and $\delta^{13}C$ from −25.7 to 3.18 ‰. On the plot of δ^2H and $\delta^{18}O$, LMWL is given by the equation: $\delta^2H=8\delta^{18}O+6.4$ (Deák et al. 1987) (Fig. 3). The temperature of the samples on the LMWL ranges from 10 to 96 °C. Samples off the LMWL are geothermal waters with temperatures up to 98 °C; Cl^--dominated geothermal samples are located in aquifers above elevated basements all over the study area, while HCO_3^--type samples with lower Cl^- are in deep sub-basins. Although the major ion chemistry in the HCO_3^--dominated samples off the LMWL is similar, the stable isotope δ values and the geographical location split them into two subgroups: one is located in the Duna-Tisza interfluve and South Tisza basin, the other is in the Körös basin. The two basins are separated by a SE–NW basement high (Fig. 1a).

On the LMWL, the type of groundwater below 30 °C changes from $Ca/Mg(HCO_3)_2$ to $NaHCO_3$, and above 30 °C it is $NaHCO_3$. The frequency distribution of their alkalinity (Fig. 4) reveals four groups: two of them can be modeled with a Gaussian probability density function, but no simple-shaped curve can be fitted to the other two. The average alkalinity of the four groups is 5.6, 9.1, 15.2, and 24.2 meq/l, respectively. The relationship between the major mono- and bivalent cations is displayed in Fig. 5, where the groups correspond to those separated on the basis of the frequency distribution of alkalinity (Fig. 4). In three of the four groups the change of the mono- and divalent cations is opposite and equivalent, indicating ion exchange. In the fourth group, the concentration of mono- and bivalent ions is independent, and the concentration of the bivalent cations is low. The mean concentrations of the Li^+, K^+, NH_4^+ and COD increase together with the mean alkalinity. The average concentrations of Cl^- in the four groups are 5.2, 8.8, 24.9 and 20.5 mg/l, respectively. Within the groups, samples with a similar alkalinity but distinct Cl^- concentration represent different regions. The Cl^- concentrations are significantly lower in the western and higher in the northern and eastern parts of the study area.

The diverse isotopic signatures and the highly variable chemical composition, including the major and trace components, show that the study area comprises different types of water; hence, for further evaluation, a separation of the homogeneous groups of water is necessary. In order to separate them, two aspects were considered: the origin of water indicated by water stable isotopes, and the chemical composition.

Discussion

The $\delta^{18}O$ and δ^2H values, the concentration of major ions, minor and trace elements, alkalinity and the relationship between the major mono- and bivalent cations are discussed next to reveal the spatial chemical patterns and to describe the groundwater bodies and the flow systems. Stuyfzand (1999) defined the water body as a coherent 3D unit of subsurface water with a specific origin. In the present work, a water body is defined as a coherent 3D unit of subsurface water of a specific origin, in which the chemical reaction controlling the concentration of the
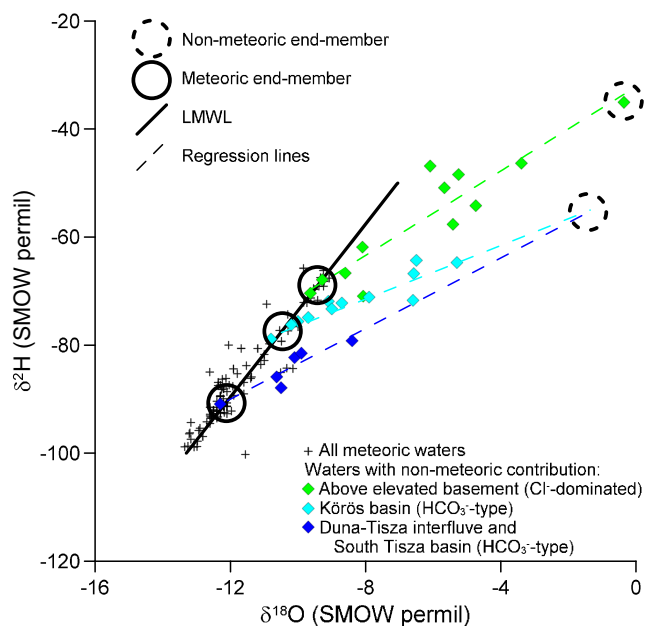
Fig. 3 Distinction between meteoric and non-meteoric waters. Samples that deviate from the local meteoric water line (LMWL) are located along three lines, each corresponding to a particular geographical unit. These samples have a non-meteoric contribution

major ions is the same all over the unit. According to this definition, a water body may consist of more than one chemical type of water, but if that is the case, the transition between them is continuous.

Mixing of meteoric and non-meteoric end-members

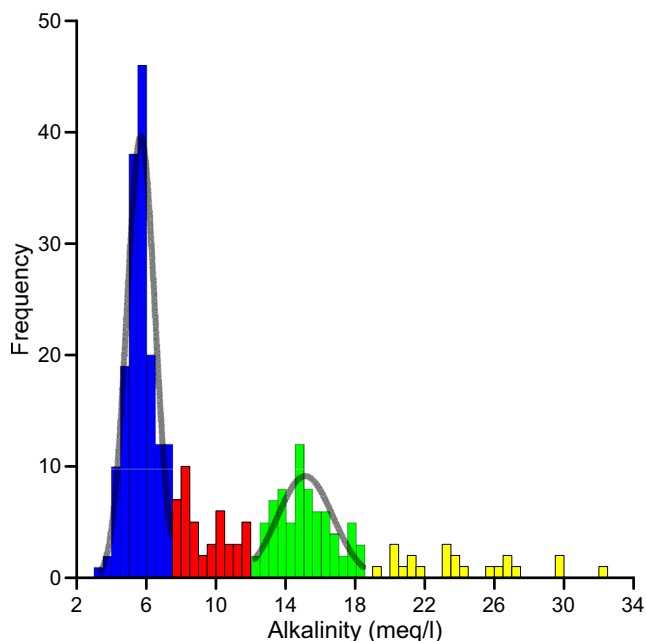Water samples on the LMWL are of meteoric origin, while those that deviate from the LMWL may be of meteoric or

Fig. 4 Frequency distribution of alkalinity in the water samples of meteoric origin. The graph reveals four distinct groups of groundwater
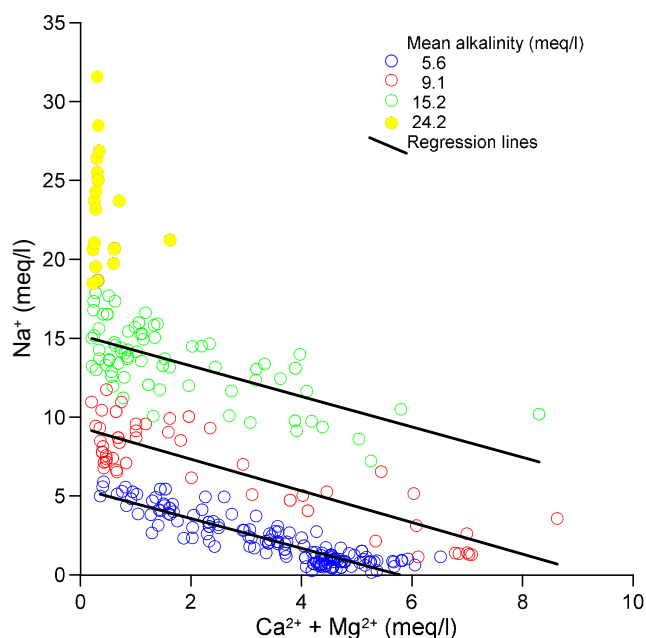
Fig. 5 Relationship between the major mono- and bivalent cations in the groups defined by the frequency distribution of alkalinity. The mirror image of the mono- and bivalent cations suggests ion exchange

non-meteoric origin. Mixing, isotope exchange at high temperature and evaporation result in deviation from the LMWL (Clark and Fritz 1997). The isotope exchange is not relevant in the study area, because samples with equally high temperature (up to 96–98 °C at the wellhead) are located both on and off the LMWL. Due to the Br to Cl ratio similar to the seawater (molar ratio: 1.6×10^{-3}) evaporation of meteoric water can be excluded as well (Varsányi and Kovács 2009). Consequently, the samples off the LMWL (Fig. 3) are mixed water with sea contribution. They seem to be located on three mixing lines. One of them consists of samples above the elevated basement including samples along the A–B trace (Fig. 1a), one is located in the Duna-Tisza interfluve and South Tisza basin, and the third one in the Körös basin (both along the C–D trace). In each group the $\delta^{18}O$ and $\delta^{2}H$ values (Fig. 3) and the Cl^- concentrations support the mixing theory. Results of geochemical modeling published elsewhere (Varsányi and Kovács 2009) verified that the non-meteoric end member was evaporated brackish water, but in the deep sub-basins probably ultrafiltration resulted in further modification in the δ values. To better understand the relevant processes, the database was extended with archival Cl^- data from deep layers lying below the producing thermal water wells.

Above the elevated basement, depth-dependence of the Cl^- provides information on the mixing of non-meteoric water with a high Cl^- concentration, and meteoric water with low Cl^- (Fig. 6a). In the deepest samples, the Cl^- concentrations are highly variable; going upward the range of variability decreases because the maximum values continuously diminish. This pattern reflects the superposition of two mixing processes—one is recorded

by the scatter of Cl⁻ at similar depth, and the other by the upward tightening of its range. The sea contribution can be traced up to a depth of 400 m. Based on the chemical pattern, the two mixings might have occurred in diverse periods of the basin's evolution: the earlier one was a dilution of the in situ seawater trapped in the deepest Pannonian sediments by the infiltrating paleometeoric water, and the later one was a mixing of the ascending deep water containing Cl⁻ in various concentrations with the in situ meteoric pore content of low Cl⁻ concentration. These two steps of the mixing occurred in different hydraulic regimes: the earlier mixing was connected to recharge and the later one to discharge. The earlier mixing process in the deepest Pannonian layers is explained on the basis of the basin evolution models of Almási (2000) and Juhász et al. (2002): by the end of the pre-Pannonian, sedimentation in the deep brackish Lake Pannon compressional stress resulted in uplift and subaerial exposure, and through the shear zones of the uplifted highs meteoric water entered the sediments. Variation of the Cl⁻ concentration indicates various proportions of mixing between the pore content of sea origin and paleometeoric water during the early burial. The entry of meteoric water into the Pannonian sediments was established by Mátyás and Matter (1997). They recognized the impact of meteoric water based on secondary porosity, feldspar leaching and kaolinite formation. Later on, in the early Pannonian, the conditions changed, thermal subsidence accompanied by rapid sedimentation led to the cessation of the meteoric influence. The next mixing process can be understood on the basis of the pressure-elevation profile. This was constructed (Fig. 7a) to display the vertical pressure distribution in the vicinity of a water well containing Cl⁻ in high concentration. The profile is a straight line; the superhydrostatic (10.04 MPa/km) vertical pressure gradient indicates an upward driving force in accordance with the Cl⁻ pattern, which shows the mixing of the ascending water with the in situ pore content of meteoric origin. On the mixing lines (Fig. 3), the meteoric end-members

belong to this second mixing process. Since the position of a sample on the MWL is connected to the temperature during infiltration (Clark and Fritz 1997), the different positions of the meteoric end-members reveal dissimilar temperatures during infiltration, and consequently, diverse periods of infiltration.

The upward-moving water goes through the Algyő Formation, which is a regional aquitard, but sedimentological discontinuities, faults and fractures locally give it an aquifer character (Tóth and Almási 2001). The aquifer character of the Algyő Formation explains the matching chemical and pressure patterns; that is, it explains the vertically continuous decrease of both the pressure-elevation profile and the envelope of the Cl⁻ concentrations (Figs. 6a and 7a).

The other two groups of the mixed water are located in sub-basins. In the Körös basin, a sharp break in the depth-dependence of Cl⁻ (Fig. 6b) and in the pressure-elevation profile (Fig. 7b) can be recognized within the Algyő Formation at about the same depth (note that the vertical axis in Fig. 6 is depth and in Fig. 7 is elevation). Below the break, the Cl⁻ fluctuates in a wide range: the maximum values exceed 300 mmol/l and the concentrations are independent of the depth, whereas above the break, the concentrations are two orders of magnitude lower than below it. Variation of Cl⁻ in the deepest Pannonian layers can be explained in the same way as in the area above the elevated basement: the water of sea origin trapped in the Pannonian sediments mixed with paleometeoric water after burial. Interpretation of the pressure-elevation profile (Fig. 7b) helps us to understand the differences of the Cl⁻ patterns above the elevated basement and the Körös basin area. The bottom segment of this profile indicates a strong overpressure, while the top segment's gradient is slightly superhydrostatic (9.94 MPa/km). In general, the Algyő Formation at the top of the Pannonian consists of mudstones, siltstones and argillaceous marl strata, and has an aquitard character. It is known that compacted clays can act as a membrane, and
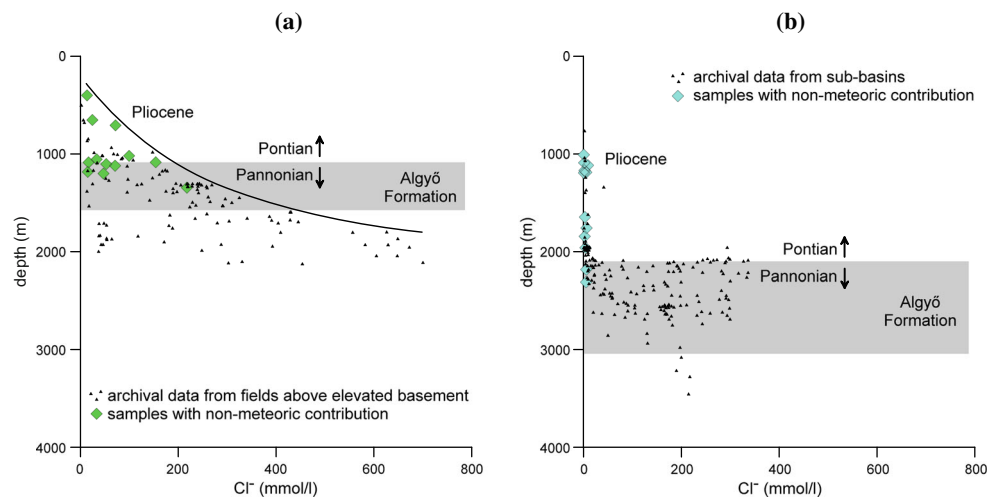

Fig. 6 Vertical distribution of Cl⁻. **a** Elevated basement (cross-section *A–B*). **b** Körös basin (cross-section *C–D*). The Cl⁻ pattern is controlled by the permeability of the Algyő Formation
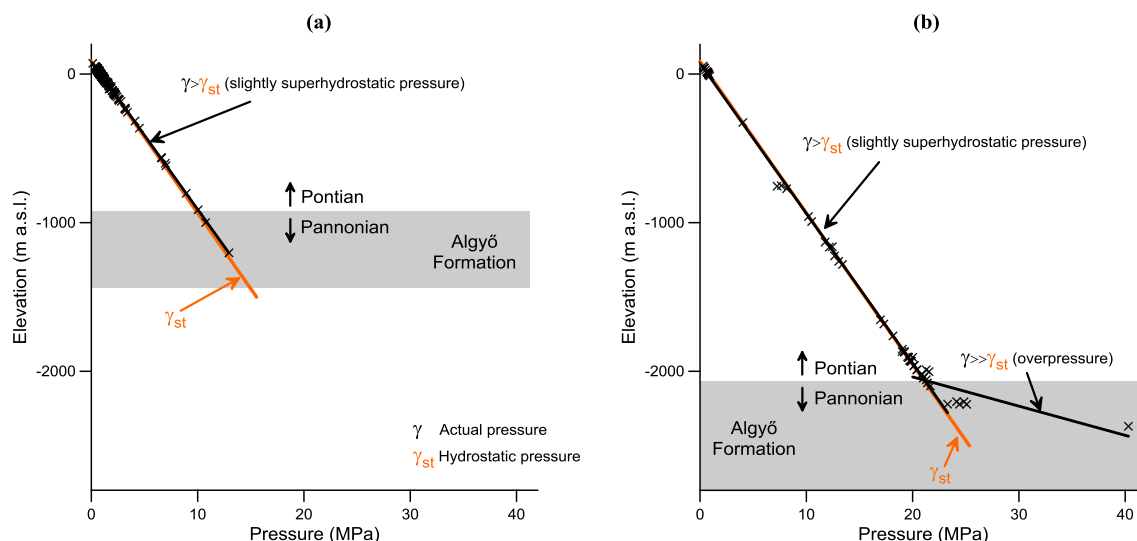
Fig. 7 Pressure–elevation profiles. **a** Elevated basement (cross-section *A–B*). The pressure gradient is uniform due to the leaky nature of the Algyő Formation. **b** Körös basin (cross-section *C–D*). The sharp break in the pressure gradient is caused by the low permeability of the Algyő Formation

that the membrane's behaviour may have an effect on the migration of solutes through such clay barriers, restricting the passage of solute (Malusis et al. 2003). The overpressure squeezes the deep water through the Algyő Formation, while the bulk of the Cl^- remains and accumulates below. In the non-meteoric end-member the modification of the isotopic δ values compared to that of the area above the elevated basement, the sharp break and the Cl^- retention are attributed to the membrane property of the compacted clays in the Algyő Formation. In this sub-basin, the non-meteoric contribution is detected to a depth of 1,000 m. Above 1,000 m, chemical and isotopic data are only available in three samples (all of meteoric origin) between 950 and 679 m. All over the Körös basin, the pressure gradient exceeds the hydrostatic one, which indicates an upward-driving force in the whole studied depth interval. No present recharge area of the meteoric water was traceable.

In the Duna-Tisza interfluve and South Tisza basin, the contribution of the deep, non-meteoric water can be detected only at the Pannonian-Pontian boundary. Unfortunately, Cl^- data from the Pannonian layers are not available, but there are two elevation-pressure profiles published by Tóth and Almási (2001; see their Figures 9 and 10), one for the flanks and another for the centre of the sub-basin. On the flanks, a normally pressured upper section and recharge from the surface down to the Pontian-Pannonian boundary (at about 1,000 m) were demonstrated. In the central part of the sub-basin, the profile indicates ascending water from a depth of about 2,500 m, which here corresponds to the depth of the Algyő Formation. In both profiles, overpressure is observed in the pre-Pannonian and the Pannonian sediments. The available scarce data affirm the possibility of a contribution of non-meteoric water arriving from the Pannonian, a flow regime which is reported by Tóth and Almási (2001); namely, infiltration at the edge of the sub-basin, lateral flow and discharge in the central part of the

sub-basin. This flow pattern explains the difference between the two basins in the distribution of the non-meteoric water: in the Duna-Tisza interfluve and South Tisza basin, the non-meteoric water was flushed in the bulk of the Pontian sediments, except the deepest layers at the Pannonian-Pontian boundary.

Processes in the water of meteoric origin

The equilibrium dissolution of the carbonates limits the Ca^{2+} and Mg^{2+} concentrations within the ranges from 2 to 111 mg/l and from 0.4 to 39 mg/l, respectively. The source of Na^+ is the kinetically driven weathering of silicates. As no sink is known, the upper limit of its concentration is the availability of sodium-containing silicates in the sediments. The older the water, the higher the concentration of Na^+ and alkalinity are. Four groups are distinguished with the increasing mean Na^+ and alkalinity, while the sum of Ca^{2+} and Mg^{2+} is limited in each group (Fig. 5), readily indicating that the character of the chemical reaction (kinetic or thermodynamic) determines the maximum concentration of the ions. Each group is located in mainly two regions: one is the Duna-Tisza interfluve and South Tisza basin, the other is the River Maros alluvial fan and the River Körös basin (Fig. 1), but there are sparse samples away from these two sites as well. These sparse samples are probably parts of other water bodies, but the number of the available samples is not enough to delineate those. The samples with low alkalinity originate from the Quaternary, with middle alkalinity from the Quaternary and Pliocene, and with high alkalinity from the Quaternary, Pliocene and Pontian layers. Within these groups, the concentration of Na^+ changes inversely and more or less equivalently to the concentration of the bivalent cations. The fourth group, the one with the highest alkalinity, consists of geothermal water from the Pontian layers. In these samples, the

concentration of Na$^+$ is independent of those of Ca^{2+} and Mg^{2+} (Fig. 5).

The Duna-Tisza interfluve and South Tisza basin
Alteration of the alkalinity in the samples from the Quaternary, Pliocene and Pontian layers is displayed from west to east in Fig. 8. In the Quaternary layers, three groups (low, middle and high alkalinity) are distinguished, corresponding to Fig. 4. From west to east, the mean alkalinity of the groups increases. In the group where alkalinity is the lowest, Na$^+$ increases, Ca^{2+} and Mg^{2+} decrease together with the decline of the surface elevation from 139 to 78 m a.s.l. Thus, the highest elevation coincides with the lowest concentration of Na$^+$. Scattering of the values is moderate, probably due to the significant flow rate. All samples with low alkalinity, mostly from the Quaternary layers, belong to the same water body because it forms a coherent unit of water with a similar meteoric origin, and the main reaction controlling the pattern of the major cations is ion exchange over the entire region where these samples are located. At the same time, this water body is a flow system in the sense defined by Tóth (1963). The recharge area is the Duna-Tisza interfluve and the discharge area is the South Tisza basin (Erdélyi 1979). Depletion of ^{18}O (Fig. 8) and ^{2}H towards the water flow suggests that infiltration occurred in a warming environment. According to the noble gas temperature, the infiltration started in cold climatic circumstances (average temperature: 3.3 °C) and continued in warming up conditions to an average of 12.9 °C in the Holocene. The change of δ^{18}O from −13.4 to −9.0 ‰, and of δ^{2}H from −98.9 to −64.6 ‰ corresponds to a 9.6 °C increase in temperature (Varsányi et al. 2011).

The question is whether the further two groups in the Quaternary, those with middle and high mean alkalinities, are parts of the flow system delineated in the preceding, or if they represent independent water bodies or flow systems. To answer the question, Cl$^-$, δ^{18}O and δ^{2}H are evaluated. In similar sedimentary environments, Cl$^-$ is a conservative parameter because it is not involved in chemical reactions, so its concentration is indicative of the origin of water, while the location of the samples on the LMWL is in connection with the temperature during infiltration. Going from west to east, the noticeable enrichment of ^{18}O (Fig. 9) and ^{2}H between the low and middle and between the middle and high alkalinity groups, and the increase of Cl$^-$ between the middle and high alkalinity groups (Fig. 10) provide evidence that the middle and high alkalinity groups are not parts of the flow system, but they correspond to distinct water bodies. These last two water bodies are located in discharge areas. In the middle alkalinity samples, not only is the residence time longer than in the flow system, but the enrichment of the heavier isotopes shows that infiltration occurred in a period which was warmer than the last glacial maximum (LGM). The elevated alkalinities suggest longer residence time. Permanent recharge of these water bodies from areas out of the study area can be excluded, because the S–N parallel pattern of the hydraulic head contours indicates W–E flow direction (Varsányi et al. 2011) and only one
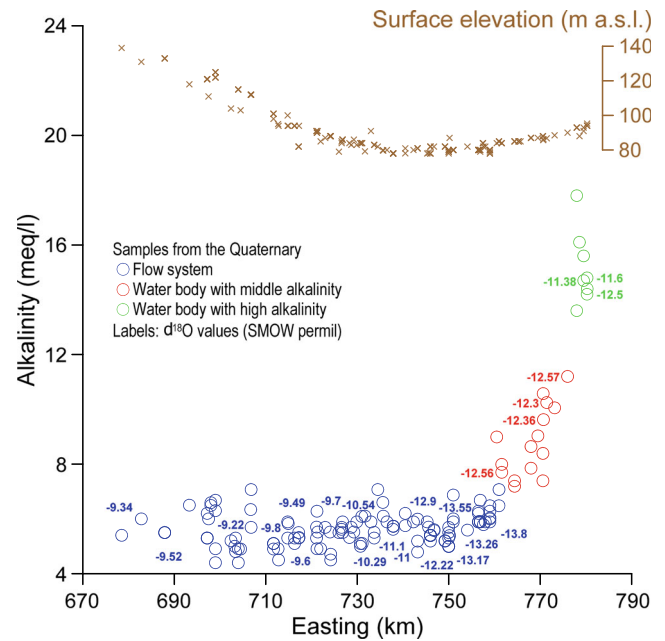

Fig. 8 Change of alkalinity and surface elevation from W to E in the Duna-Tisza interfluve and South Tisza basin for three distinct groups of water in the Quaternary layers. The group with the lowest alkalinity forms a flow system. In the two water bodies, the higher alkalinities may be due to longer residence times

possible recharge area in the Duna-Tisza interfluve. In the low alkalinity flow system at the end of the flow path, the mean δ^{18}O is −13.2 ‰, while in the middle and high alkalinity samples it is −12.4 and −11.79 ‰, respectively; thus, it seems probable that the water bodies of middle and high alkalinity were recharged before the start of the infiltration of the low alkalinity flow system during the last glacial period. A certain change in the hydraulic circumstances initiated infiltration in the present recharge area and the flow system of low alkalinity nested in the former water body, which remained in the sediments eastward from and below the developing present flow system. Because of the chemical and isotopic similarity, several samples from the Pliocene layers seem to belong to this discharging water body (Fig. 9). The upward moving water in the Pliocene merges with the discharging water in the Quaternary, and they form one water body. The Quaternary water samples with high alkalinity form a further distinct water body, in which the elevated Cl$^-$ and the (sparse) stable isotope data provide support that the source of this water body differs from that of the previous one.

Despite the upward-driving force acting up to the surface, the vertical distribution is similar to that of the recharge section of the low alkalinity flow system, i.e. Ca^{2+} and Mg^{2+} increase towards the surface in the two last water bodies. To explain the upward increase of Ca^{2+} and Mg^{2+} in the discharging water, it is assumed that at least a part of the region previously functioned as a recharge area, where equilibrium dissolution of carbonates occurred, and the predominant cations were Ca^{2+} and Mg^{2+}. Equilibrium between the Ca^{2+} and Mg^{2+} type water and clay minerals resulted in Ca^{2+} and Mg^2 exchange complexes on the
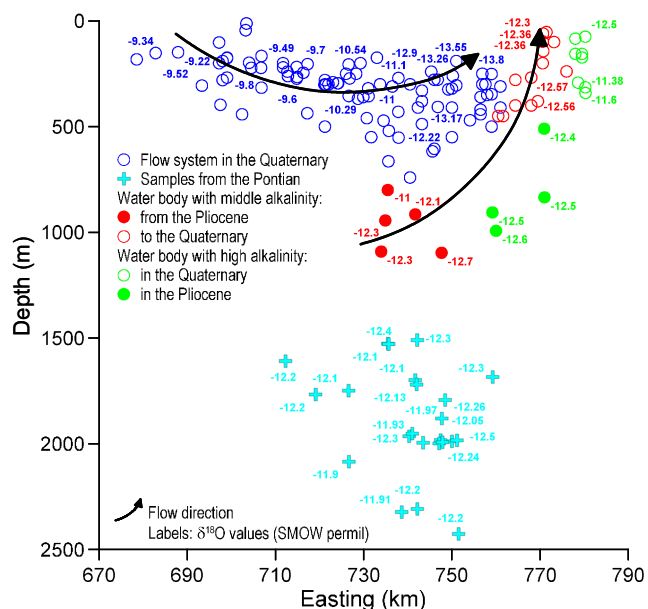
Fig. 9 Flow directions concluded from the chemistry in the Duna-Tisza interfluve and South Tisza basin. The pathways are indicated by the increase of Na^+ and decrease of the bivalent ions

clay minerals. Due to the change of the hydraulic circumstances, the infiltration ceased. Additional CO_2 was produced by the transformation of organic matter, but without raising the partial pressure of CO_2. Consequently, the weathering of the Na-silicates proceeded and raised the concentration of Na^+ in proportion to the residence time, but without further dissolution of the carbonate minerals. Ion exchange occurred between the upward moving Na^+ type water and the exchangeable Ca^{2+} and Mg^{2+} on the clay minerals, and the new
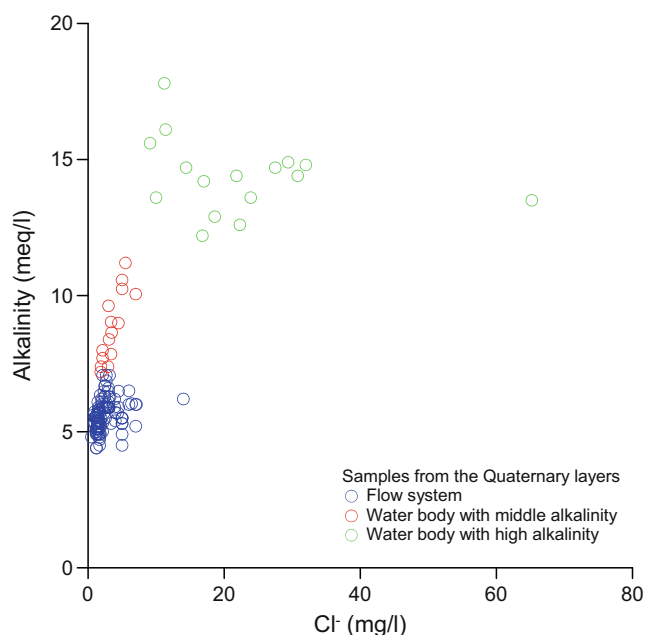

Fig. 10 Relationship between alkalinity and Cl^- in the Duna-Tisza interfluve and South Tisza basin. The water body with high alkalinity is separated on the basis of the high Cl^- concentrations

equilibrium resulted in an increase of Ca^{2+} and Mg^{2+} in the water; therefore, it can be concluded that the upward increase of Ca^{2+} and Mg^{2+} together with the elevated alkalinity may be indicative of an alteration of the hydraulic regime in a given area. Moreover, the change of the hydraulic conditions might have initiated the flow of the deep, old, Na^+ type water towards the surface and the exchange of dissolved Na^+ to Ca^{2+} and Mg^{2+} as well.

Tóth and Almási (2001) published a hydraulic cross-section (E–F trace; Fig. 1a,) close to the trace of the C–D line through the sub-basins shown in Fig. 1c and, thus, one can compare the chemical (Fig. 11a) and the flow (Fig. 11b) patterns in the Duna-Tisza interfluve and the South Tisza basin. Although, except for the western flank, the hydraulic cross section shows a consistent upward driving force up to the shallowest layers, the isolation of a water body from the nearby and underlying ones testifies to a break in the upward flow. It seems as if a boundary separates the nested flow system of low alkalinity from the accommodating water body with a higher alkalinity. As the present boundary was developed at a certain time when the circumstances were favorable for starting up ion exchange, the boundary is not permanent, so on the geological time scale the inconsistency between the hydraulic and chemical patterns is provisional.

In contrast to the flow system discussed in the previous, in the geothermal samples originated from the Pliocene and Pontian layers, the range of the $\delta^{18}O$ and δ^2H values covers a surprisingly narrow interval (Fig. 12). The stable isotope δ values of the geothermal water are less negative than those of the samples from the end part of the Quaternary flow system, which infiltrated during the last glacial maximum (LGM); therefore, recharge of the geothermal water occurred either before or after the LGM, probably in warmer temperature conditions than during the LGM. To decide if the geothermal water is older or younger than the groundwater, which infiltrated during the LGM, the concentration of Li^+, being an indicator of residence time, and the δ values were considered.

Residence time indicators are those components where the concentration is proportional to the residence time of water (for example, Li^+, K^+, Na^+), because they are products of kinetically controlled reactions (Edmunds and Smedley 2000). In the Quaternary flow system, the concentration of Li^+ is very low (<0.009 mg/l), δ^2H varies from −98.9 to −65.8 ‰ and towards the more negative δ values Li^+ is slightly increasing (Fig. 13). The conventional radiocarbon ages are increasing along the flowpath from 1,713 years to 45,868, but at the end of the flowpath the age is uncertain due to the mixing with old groundwater free of ^{14}C (Varsányi et al. 2011). The samples from the Pliocene contain Li^+ in higher concentrations (0.005–0.027 mg/l) than the Quaternary samples. The higher Li^+ indicates that the residence time is longer than in the Quaternary flow system. Consequently, the infiltration in the Quaternary started at around the LGM and proceeded in warming circumstances, whereas in the Pliocene it started before the LGM. In the Pontian layers, the concentrations of Li^+ exceed those in the Pliocene,
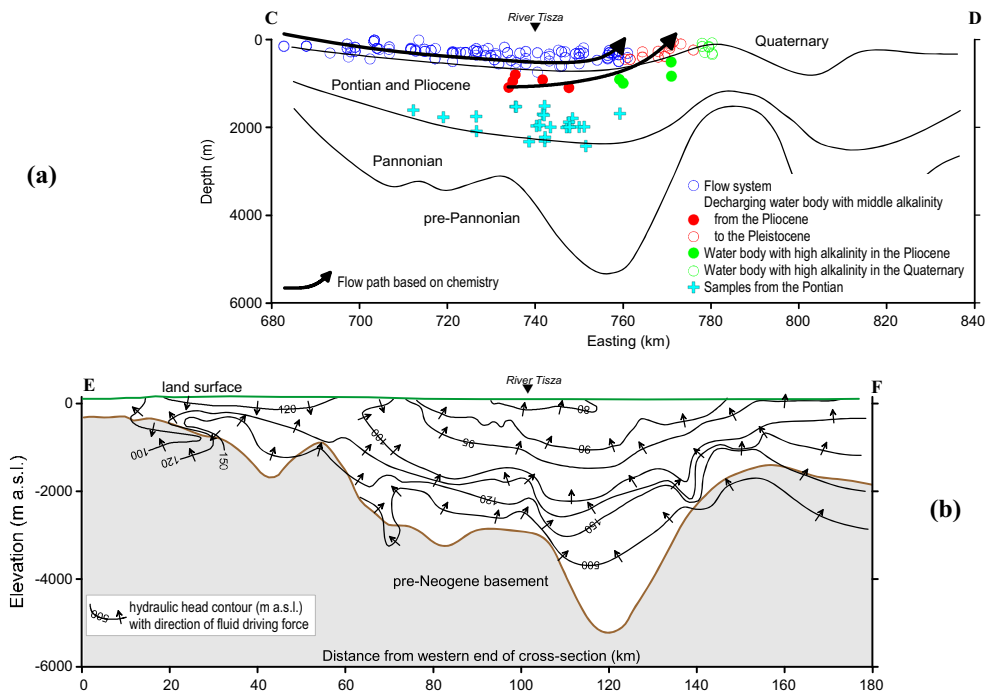
Fig. 11 Hydrogeochemistry compared with hydrology in the Duna-Tisza interfluve and South Tisza basin. **a** Suggested water bodies (cross-section *C–D*); due to the perpendicular projection of the sampled intervals of wells onto the cross-section, a few samples appear outside their stratigraphic unit. **b** Potentiometric profile (cross-section *E–F*) simplified and redrawn from Figure 20 of Tóth and Almási (2001)

indicating that in the deeper layers the residence time is even longer than in the Pliocene, so the infiltration here occurred formerly.

In the Pliocene and Pontian layers, the limited range the of δ values together with the higher NaHCO₃ and

Fig. 12 Relationship between $\delta^{18}O$ and δ^2H in the Duna-Tisza interfluve and South Tisza basin. Replenishment of the Quaternary, Pliocene and Pontian layers occurred in warmer conditions than the last glacial maximum (LGM), while recharge of the flow system in the Quaternary layers was continuous from the LGM to the Holocene

other residence time indicators show a much longer contact time and a more restricted climatic change during infiltration than the samples from the Quaternary. The distinct, vertically superimposed water bodies suggest intermittent infiltration that occurred mostly in particular time periods when the given layers were in a near-surface position and the circumstances were favorable for infiltration. K^+, Li^+ and COD support the separation of the Pontian and Pliocene layers.
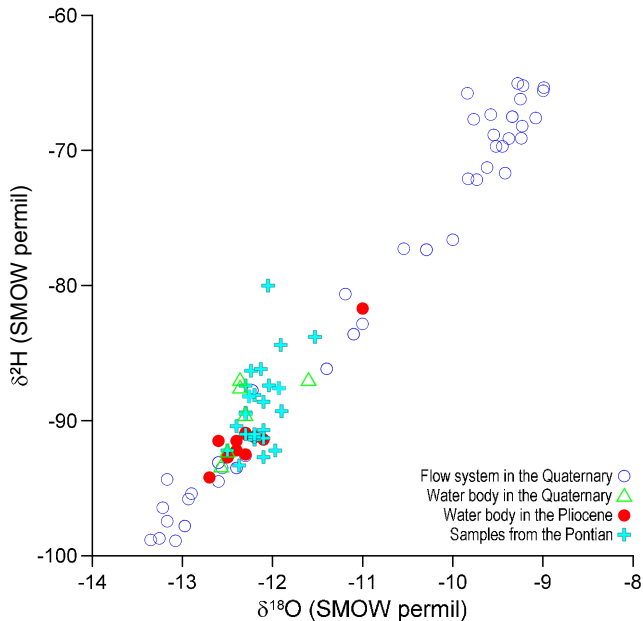
The River Maros alluvial fan and the Körös basin
The Quaternary samples from the River Maros alluvial fan are of low and middle alkalinity, and in the Körös basin it is high. The Li^+, as a residence time indicator, suggests that the samples of low and middle alkalinity form one water body in the alluvial fan, and those with high alkalinity in the Körös basin compose another (Fig. 14a and b). In the River Maros alluvial fan (Fig. 1) the surface elevation slightly descends from south to north. The increase in alkalinity from south to west, northwest and north, together with an opposite change of the mono- and bivalent ions towards these directions, indicates the direction of groundwater flow (Fig. 15), but the correlation between the mono- and bivalent ions is much less significant than in the Duna-Tisza interfluve and South Tisza basin. In the southern part of the River Maros alluvial fan, at the state boundary where the surface elevation is the highest, the proportion of Ca^{2+} and Mg^{2+} to Na^+ is lower than in the recharge area in the Duna-Tisza interfluve in spite of the similar alkalinity, suggesting that
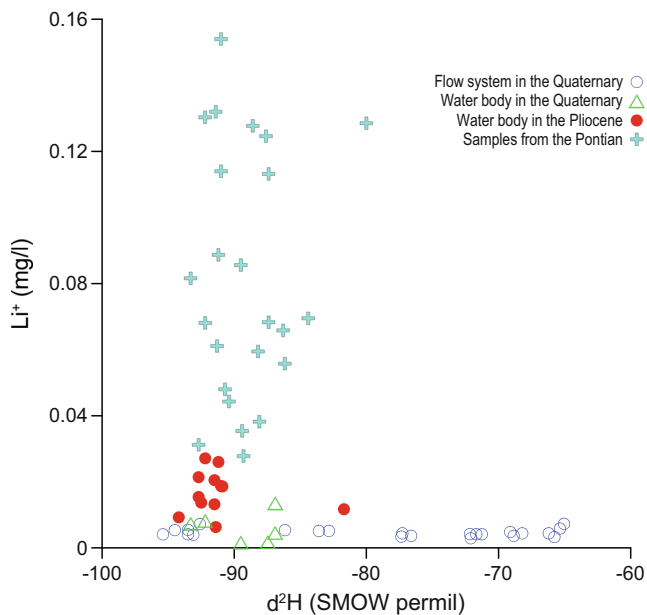
Fig. 13 Relationship between Li$^+$ and δ^2H in the Duna-Tisza interfluve and South Tisza basin. Li$^+$, as a residence time indicator, suggests a shorter residence time in the complete flow system than in the water bodies, indicating that infiltration of water bodies occurred before the LGM

this is the throughflow segment of the flow paths, which means the infiltration occurred outside the state border, which is in accordance with the hydrodynamic circumstances demonstrated by Erdélyi (1979); the recharge area of the River Maros alluvial fan is south of the Hungarian
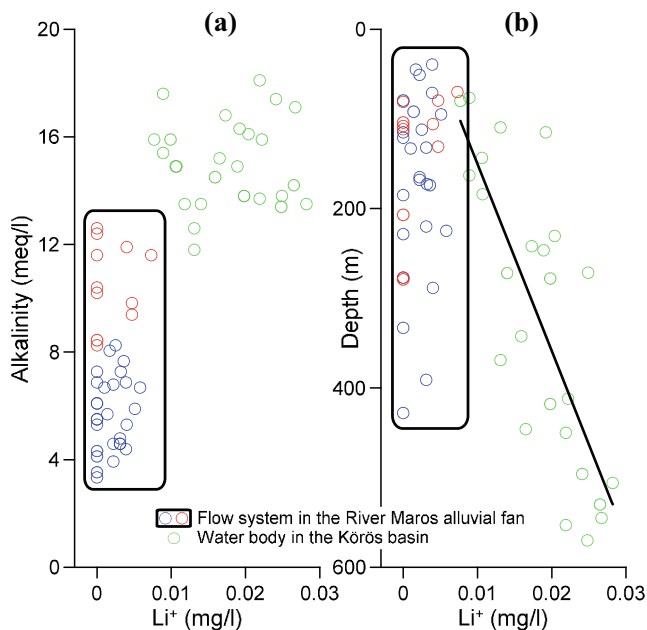

Fig. 14 Alkalinity and Li$^+$ in the River Maros alluvial fan and the Körös basin. **a** Relationship between alkalinity and Li$^+$. **b** Vertical distribution of Li$^+$. On the basis of these relationships, two groups of samples are distinguished in the Quaternary layers: one in the River Maros alluvial fan, where samples with low (*red circles*) and middle (*blue circles*) alkalinities compose a flow system, and the other, a water body in the Körös basin
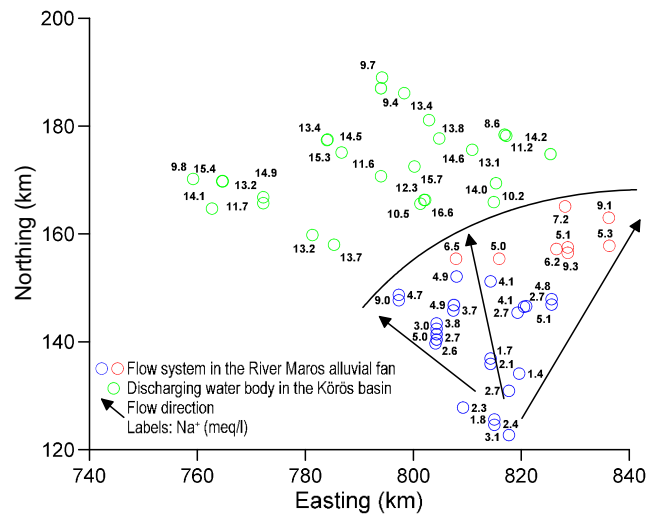

Fig. 15 Wells in the River Maros alluvial fan and the Körös basin with Na$^+$ values and suggested flow lines. In the River Maros alluvial fan samples with low (*red circles*) and middle (*blue circles*) alkalinities compose a flow system, while in the Körös basin, a water body with high alkalinity is found. In the River Maros alluvial fan, flow directions correspond to increasing Na$^+$

state border (Fig. 1). The increasing alkalinity towards the flow direction shows that in the River Maros alluvial fan the most important chemical reactions controlling the major ion chemistry are the weathering of Na-silicates and ion exchange. Although the recharge area is out of the study area, this water body is a south to west, northwest and north flow system as well, where the samples of low alkalinity are located in the throughflow segment and the samples of middle alkalinity correspond to the end of the flow path. The chemical feature of the high alkalinity water located in the Körös basin (Fig. 14a and b) indicates that this is a distinct discharging water body with a much longer residence time than in the River Maros alluvial fan. The elevated alkalinity is attributed to the break of the infiltration in a former recharge area due to a certain alteration in the hydraulic circumstances, which has resulted in the increase of residence time.

Conclusions

Following the evaluation and interpretation of the δ^{18}O and δ^2H values, the chemical data and the fluid potential pattern, taking the chemical principles, geology, pressure conditions and evolutionary history of the area into account, the general conclusions of this work are as follows.

Distinct water flow systems and water bodies can be distinguished on the basis of water chemistry, including isotopes. In certain parts of the study area, these flow systems and water bodies seem to be separated from each other in spite of the region's hydraulic continuity. The flow path within the flow systems and water bodies is recorded by the chemical composition, but in different circumstances, different chemical components are relevant.

In some places, Cl$^-$ concentrations, together with δ^{18}O and δ^2H, are useful tracers for water flow. In the study

area below the Pannonian-Pontian boundary, the deep water has a significant non-meteoric contribution, which was trapped in the sediments during deposition in the brackish Lake Pannon. The Cl⁻ concentration is high and the upward decreasingly high Cl⁻ concentrations confirm the upward flow of deep water, which is suggested by the pressure gradient exceeding the hydrostatic one, as well.

In another places vertical hydraulic communication through an aquitard is evidenced. The overpressure below the aquitard is an upward driving force. The sudden drop of the Cl⁻ above the aquitard indicates that the water below has squeezed through compacted clays, which acted as a membrane, and the bulk of the Cl- remains and accumulates below.

In spite of the overall slightly superhydrostatic pressure gradient, the discharging water forms distinct water bodies in the Pontian and in the overlying Pliocene and Quaternary. The lack of the present recharge flow regime reveals that replenishment had occurred in previous time periods. Afterwards, the infiltration ceased due to the alteration of hydraulic circumstances. Cessation of the infiltration resulted in an increase of the residence time, which is recorded by certain ions like HCO_3^-, Na^+ or Li^+, because their concentration is kinetically controlled. All of this suggests that the present chemical composition of subsurface water may record past geological environments and events.

The chemical pattern in the study area is very similar to the Chebotarev sequence, as the total dissolved solids (TDS) in the recharging shallow water is low, the dominant anion is HCO_3 and the dominant cation is Ca^{2+}; with increasing depth TDS and Na^+ concentrations increase, Ca^{2+} decreases, and in the deepest layers Cl^- is the dominant anion. Nevertheless, the Chebotarev pattern is attributed to the basin's evolution instead of to the chemical evolution of subsurface water along one flow path from the recharge to the discharge. Alteration of the surface elevation, uplift and subsidence in different periods and places, together with alteration of the sedimentary environment and the depth of burial during infiltration determine the chemical pattern of the subsurface water. All these alterations can be explained by the basin evolution model, which reveals that the regional Chebotarev sequence is composed of distinct flow systems and water bodies of different origins, independent infiltration and chemical evolution. The chemical pattern suggests that the pore pressure propagation does not imply effective and continuous fluid flow over a geological time scale.

References

Almási I (2000) Petroleum hydrogeology of the Great Hungarian plain, Eastern Pannonian Basin, Hungary. PhD Thesis, University of Alberta, Department of Earth and Atmospheric Sciences, Edmonton, AB, Canada

Appelo CAJ, Postma D (1993) Geochemistry, groundwater and pollution. Balkema, Rotterdam, The Netherlands

Back W (1966) Hydrochemical facies and groundwater flow patterns in Northern part of Atlantic Coastal Plain. US Geol Surv Prof Pap 498-A

Back W, Hanshaw BB (1970) Comparison of chemical hydrogeology of the carbonate peninsulas of Florida and Yucatan. J Hydrol 10:330–368

Chebotarev II (1955) Metamorphism of natural waters in the crust of weathering: 1. Geochim Cosmochim Acta 8:22–48

Clark I, Fritz P (1997) Environmental isotopes in hydrogeology. Lewis, New York

Deák J (2006) A Duna-Tisza köze rétegvíz áramlási rendszerének izotóp hidrológiai vizsgálata [Isotope hydrological study of the groundwater flow regime of Danube-Tisza region] (In Hungarian). PhD Thesis, Eötvös Loránd University, Budapest, Hungary

Deák J, Stute M, Rudolph J, Sonntag C (1987) Determination of the flow regime of Quaternary and Pliocene layers in the Great Hungarian plain (Hungary) by D, ¹⁸O, ¹⁴C, and noble gas measurements. International Symposium on the Use of Isotopes Techniques in Water Resources Development, IAEA, Vienna, 30 March–3 April 1987

Edmunds WM, Smedley PL (2000) Residence time indicators in groundwater: the East Midlands Triassic sandstone aquifer. Appl Geochem 15:737–752

Erdélyi M (1979) Hydrodynamics of the Hungarian basin. VITUKI Proceedings, Budapest, 1979

Horváth F, Cloetingh S (1996) Stress-induced late stage subsidence anomalies in the Pannonian Basin. Tectonophysics 266:287–300

Horváth F, Pogácsás Gy (1988) Contribution of seismic reflection data to chronostratigraphy of the Pannonian Basin. In: Royden L, Horváth F (eds) The Pannonian Basin. AAPG Memoir 45, Tulsa, OK, pp 97–107

Juhász A, Tóth MT, Ramseyer K, Matter A (2002) Connected fluid evolution in fractured crystalline basement and overlying sediments, Pannonian Basin, SE Hungary. Chem Geol 182:91–120

Magyar I (2010) A Pannon medence ősföldrajza és környezeti viszonyai a késő miocénben [Paleogeography and environmental conditions of the Pannonian Basin in the Late Miocene] (in Hungarian). Geolitera, Szeged, Hungary, 140 pp

Malusis MA, Shackelford CD, Olsen HW (2003) Flow and transport through clay membrane barriers. Eng Geol 70:235–248

Mátyás J, Matter A (1997) Diagenetic indicators of meteoric flow in the Pannonian Basin, southeast Hungary. In: Montanez IP et al (eds) Basin wide diagenetic patterns: integrated petrologic, geochemical and hydrologic considerations. Soc Econ Paleontol Mineral Spec Publ 57:281–296

Nagymarosy A, Hámor G (2012) Genesis and evolution of the Pannonian Basin. In: Haas J (ed) Geology of Hungary. Springer, Heidelberg, pp 149–200. doi:10.1007/978-3-642-21910-8

Ophori DU, Tóth J (1989) Patterns of ground-water chemistry, Ross Creek Basin, Alberta, Canada. Groundwater 27:20–26

Sacchi M, Horváth F (2002) Towards a new time scale for the upper Miocene continental series of the Pannonian Basin (central Paratethys). EGU Stephan Mueller Spec Publ Ser 3:79–94

Stuyfzand PJ (1999) Patterns in groundwater chemistry resulting from groundwater flow. Hydrogeol J 7:15–27

Tóth J (1963) A theoretical analysis of groundwater flow in small drainage basins. J Geophys Res 68:4795–4812

Tóth J, Almási I (2001) Interpretation of observed fluid potential patterns in a deep sedimentary basin under tectonic compression: Hungarian Great Plain Pannonian Basin. Geofluids 1:11–36

Varsányi I, Kovács LO (2009) Origin, chemical and isotopic evolution of formation water in geopressured zones in the Pannonian Basin, Hungary. Chem Geol 189:165–182

Varsányi I, Matray JM, Kovács LO (1997) Geochemistry of formation waters in the Pannonian Basin (southeast Hungary). Chem Geol 140:89–106

Varsányi I, Palcsu L, Kovács ÓL (2011) Groundwater flow system as an archive of palaeotemperature: noble gas, radiocarbon, stable isotope and geochemical study in the Pannonian Basin, Hungary. Appl Geochem 26:91–104